How to cite: *Angew. Chem. Int. Ed.* **2022,** *61,* e202209953
International Edition: doi.org/10.1002/anie.202209953
German Edition: doi.org/10.1002/ange.202209953

Helical Polymers

Full Control of the Chiral Overpass Effect in Helical Polymers: P/M Screw Sense Induction by Remote Chiral Centers After Bypassing the First Chiral Residue

*Rafael Rodríguez[+], Elena Rivadulla-Cendal[+], Manuel Fernández-Míguez, Berta Fernández, Katsuhiro Maeda, Emilio Quiñoá, and Félix Freire**

Abstract: In helical polymers, helical sense induction is usually commanded by teleinduction mechanism, where the largest substituent of the chiral residue directly attached to the main chain is the one that commands the helical sense. In this work, different helical structures with different helical senses are induced in a helical polymer [poly-(phenylacetylene)] when the conformational composition of two different dihedral angles of a pendant group with more than two chiral residues is tamed. Thus, while the dihedral angle at chiral residue **1** [(*R*)- or (*S*)-alanine], attached to the backbone, produces an extended or bent conformation in the pendant resulting in two scaffolds with different stretching degree, the second dihedral angle at chiral residue **2** [(*R*)- or (*S*)-methoxyphenylacetamide] places the substituents of this chiral center in a different spatial orientation, originating opposite helical senses at the polymer that are induced through a total control of the "chiral overpass effect".

[*] Dr. R. Rodríguez,[+] E. Rivadulla-Cendal,[+] M. Fernández-Míguez, Prof. Dr. E. Quiñoá, Prof. Dr. F. Freire
Centro Singular de investigación en Química Biolóxica e Materiais Moleculares (CiQUS) e Departamento de Química Orgánica, Universidade de Santiago de Compostela
15782, Santiago de Compostela (Spain)
E-mail: felix.freire@usc.es

Dr. R. Rodríguez,[+] Prof. Dr. K. Maeda
WPI Nano Life Science Institute (WPI-NanoLSI)
Kanazawa University
Kakuma-machi, Kanazawa 920-1192 (Japan)

Prof. Dr. B. Fernández
Departamento de Química Física
Universidade de Santiago de Compostela
15782 Santiago de Compostela (Spain)

Prof. Dr. K. Maeda
Graduate School of Natural Science and Technology
Kanazawa University
Kakuma-machi, Kanazawa 920-1192 (Japan)

[+] These authors contributed equally to this work.

Introduction

During the last decade, the field of helical polymers has flourished in the preparation of new architectures with defined macromolecular structure (i.e., handedness and elongation degree) that mimic the natural ones—peptides, saccharides or nucleic acids amongst others—, drawing the attention of the scientific community for their potential applications as chiral materials.[1] It should be noted that these systems have been successfully applied in different fields such as asymmetric synthesis,[2] sensing,[3] chiroptical switches,[4] switchable chiral stationary phases for HPLC,[5] chiral templates,[6] spin filters,[7] CPL sources[8] and biological applications[9] among others. Since the applications mentioned above directly rely on the secondary structure exhibited by these macromolecules, the preparation of defined compressed/stretched scaffolds with preferred *P*/*M* handedness is a matter of great interest to obtain chiral materials with enhanced properties. Among helical polymers, poly(phenylacetylene)s (PPA)s[10] represent an appealing family of compounds where both structural features, elongation and handedness, can be modulated either separately or together by the application of proper external stimuli.[11] The adoption of a screw sense excess in a PPA can be achieved following different strategies such as supramolecular interactions with chiral or achiral moieties, as well as by the inclusion of a single chiral center with a preferred conformation at the pendant group of the polymer.[12] Remarkably, further modifications on the conformational composition of the pendant group can lead to helix induction,[13] helix inversion[14] or even to modifications on the stretching degree of the polymer backbone.[3a,15] Unfortunately, when the pendant is composed by two or more chiral centers, the one closest to the polymer backbone is most likely to control the handedness of the polymer, while the other center has low-to-null impact on the structural features of the helical structure.[16] Interestingly, our group has recently reported the "chiral-overpass" inductive mechanism. To activate such an effect, a bent conformation must be fixed at the pendant group through an external stimulus (i.e., metal cations). This geometry locates the second chiral moiety closer to the polyene backbone, now being responsible for the helical sense adopted by the polymer.[17] In this system, by changing the absolute configuration of the second chiral residue, it is possible to invert the helical sense of the PPA.

Herein we want to take a step forward by doing a selective conformational control of two different dihedral angles. Thus, while the first dihedral angle will be responsible for the activation/deactivation of the chiral overpass induction, the second dihedral angle, located on chiral residue 2, will be the cause of the *P*/*M* helical sense induced in the PPA when the chiral overpass effect is activated. To do that, we envisaged a monomer unit that combines an amino acid involved in structural motifs such as turns[4a,18] and β-sheets[4b,18] together with a conformationally switchable arylacetic acid.[11,12a,15b,19] Therefore, while playing with the conformation of the amino acid it is possible to activate (γ-turn)/deactivate (extended) the chiral overpass effect, conformational changes at the arylacetic group will position the aryl ring in opposite directions and thus inducing a *P* or an *M* helical sense at the PPA without changing the absolute configuration of the second residue (Scheme 1).

Results and Discussion

A set of monomers made up of all possible diastereoisomers of the 4-ethynylanilides of (*S*)- or (*R*)-Alanine (Ala) derivatized at the N-terminus with the two enantiomeric forms (*R*)- or (*S*)-α-methoxy-α-phenylacetic acid (MPA)—m-(*S*)-Ala-(*R*)-MPA; m-(*S*)-Ala-(*S*)-MPA; m-(*R*)-Ala-(*R*)-MPA; m-(*R*)-Ala-(*S*)-MPA—(Figure 1) were prepared following a multistep synthetic protocol (see Supporting Information).

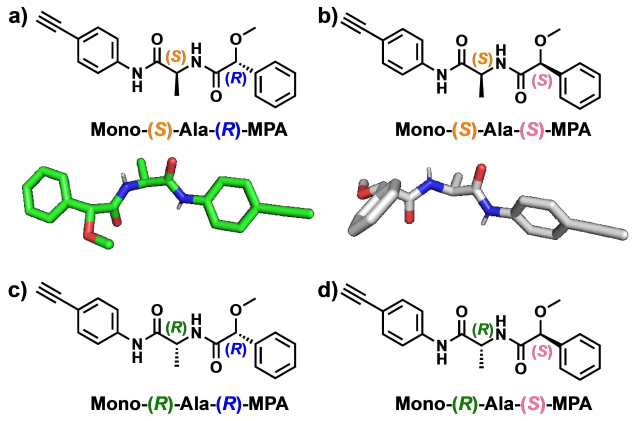

Figure 1. Structures of monomers employed in this work. a) mono-(*S*)-Ala-(*R*)-MPA and its X-Ray structure. b) mono-(*S*)-Ala-(*S*)-MPA and its X-Ray structure. c) mono-(*R*)-Ala-(*R*)-MPA and d) mono-(*R*)-Ala-(*S*)-MPA.

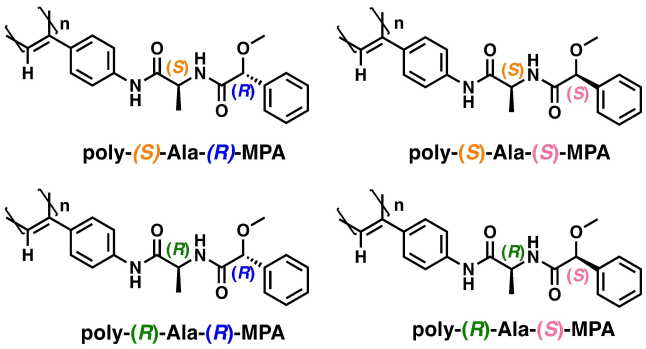

Figure 2. Structures of the polymers employed in this work.

Crystal structures of m-(*S*)-Ala-(*R*)-MPA and m-(*S*)-Ala-(*S*)-MPA were obtained, and their X-Ray studies showed extended structures of the two chiral residues (see Figures S13 and S14).[20] These monomers were polymerized using $[Rh(nbd)Cl]_2$ as catalyst,[21] which produced the corresponding polymers (Figure 2) in high yield, low polydispersity (see Table S2) and *cis*-stereoregularity of double bonds as inferred by ^1H NMR[22,23] (see Fig S15–16) and Raman (see Fig S17).[23] Differential Scanning Calorimetry (DSC) experiments showed the presence of two consecutive exothermic peaks for both polymers suggesting the adoption of *cis-transoidal* (*c-t*) stretched structures ($\omega_1 > 90°$, see Figure S18).[24]

Chiral overpass studies were then performed by ECD, UV/Vis and VCD. To carry them out, polymers poly-(*S*)-Ala-(*R*)-MPA and poly-(*S*)-Ala-(*S*)-MPA were dissolved in $CHCl_3$ and DMSO. These solvents were chosen to promote the formation and disruption of a bent structure at the pendant. Thus, while $CHCl_3$ favors a bent structure, most probably stabilized by intra-pendant hydrogen bonds to form a γ-turn mimetic motif at the pendant, DMSO disrupts these supramolecular bonds due to its interaction with the anilide groups. As a result, a β-sheet mimetic motif is generated at the pendant (extended structure).[18] ECD/UV/Vis spectra of poly-(*S*)-Ala-(*S*)-MPA in $CHCl_3$ and DMSO depict a variation in the stretching degree in total agreement with the presence of a bent and extended structure at the pendant group respectively (Figure 3b).

To corroborate the presence of this equilibrium between bent and extended structures promoted by the activation/deactivation of an intramolecular hydrogen bond, external stimuli such as F^- (added as TBAF salt) or TFA, which act as hydrogen bond disruptors,[4b,11a] were added to the $CHCl_3$ solution of poly-(*S*)-Ala-(*S*)-MPA giving rise to an ECD/UV/Vis pattern resembling that obtained in DMSO (Figure 3c). Moreover, addition of metal cations (i.e., Li^+ and Ba^{2+} perchlorates, 10 mg mL^{-1} MeOH solutions) to a solution of poly-(*S*)-Ala-(*S*)-MPA in $CHCl_3$ also promoted the adoption of compressed helices analogous to the previous ones. The reason lies in the coordination of the metal ions with the C=O groups that promote the formation of an extended structure in the pendant (Figure 3d).[13a,14b,c] Analogous studies were carried out for the other polymer counterparts displayed in Figure 2, which show the same stretching effects and opposite helical sense of the PPAs due to enantio/diastereomeric relationships (See S22 and S23).

To further corroborate that PPA compression/stretching is due to selective manipulation between a bent and an extended structure in the pendant (Figure 4a), VCD spectroscopy studies were carried out. This technique is a powerful tool in the structural elucidation of supramolecular and covalent helical polymers.[19b,25] Comparison of the VCD patterns of poly-(*S*)-Ala-(*R*)-MPA and poly-(*S*)-Ala-(*S*)-MPA in $CDCl_3$ and DMSO-d_6 reveals a totally different

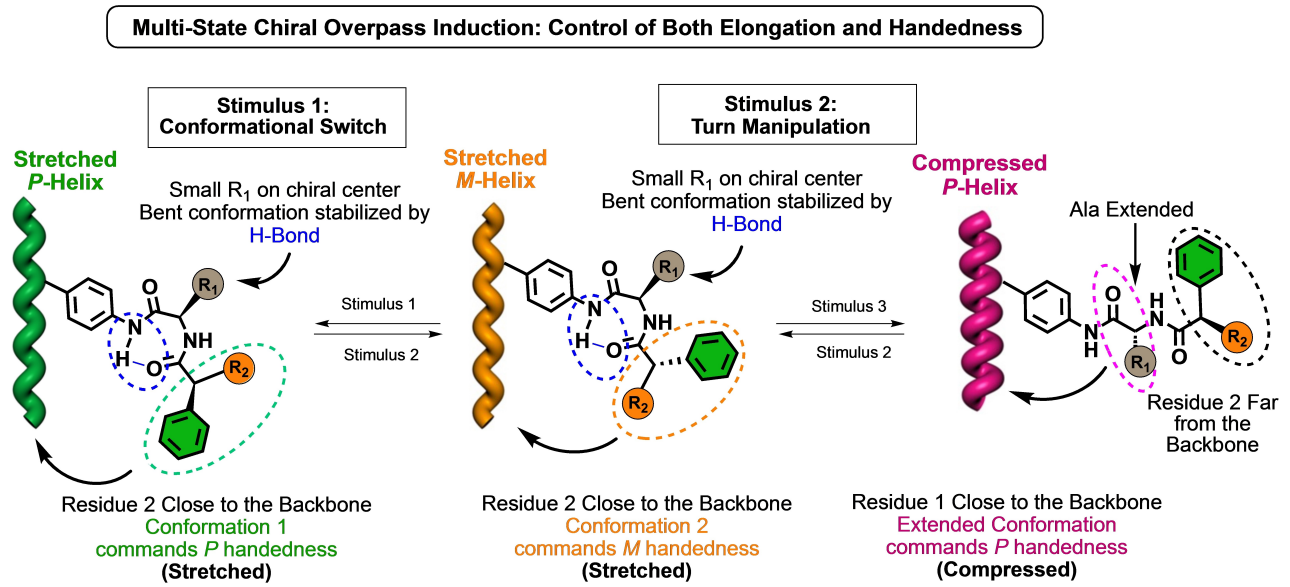

Scheme 1. Conceptual representation of multi-state chiral overpass-induction controlling both stretching and handedness.

dichroic spectra when shifting from a bent ($CHCl_3$) to an extended conformation at the pendant (DMSO) in both cases (Figures 4b and 4c).[26] Therefore, VCD is a useful technique to elucidate structural variations at the pendant group.

Computational DFT studies were carried out on monomers m-(*S*)-Ala-(*R*)-MPA and m-(*S*)-Ala-(*S*)-MPA using the wB97XD functional together with the 6–31G(d,p) basis set. As input, the structures of the monomers were introduced with a γ-turn conformation at the alanine residue. The obtained optimized geometries indicated that the chirality of the Ala promotes in the γ-turn a specific angle of −65°, independent of the absolute configuration of the second chiral center (i.e., the MPA moiety), maintaining in both cases an *ap* conformation in the MPA moiety (see Figures 5c–d and Figure S24). Comparison of the calculated γ-turn VCD pattern with the experimental ones obtained for poly-(*S*)-Ala-(*R*)-MPA and poly-(*S*)-Ala-(*S*)-MPA in $CHCl_3$ shows a good match between theoretical and experimental data, and almost identical for both polymers. This fact indicates that the VCD pattern (bisignate) observed for either poly-(*S*)-Ala-(*R*)-MPA and poly-(*S*)-Ala-(*S*)-MPA in $CHCl_3$ is governed by the presence of a bent structure at the pendant in this solvent (γ-turn a specific angle of −65°), whose −/+ sign is unaffected by the absolute configuration of the MPA moiety (Figures 5a–b).

Next, to further confirm that bent and extended conformations at the pendants have different VCD patterns, theoretical studies were carried out on mimetics of multi-parallel β-sheet motifs of mono-(*S*)-Ala-(*R*)-MPA and mono-(*S*)-Ala-(*S*)-MPA (see Figure S24). These studies show a good match between theoretical—using B3LYP functional with the 6-31G(d,p) basis set—and experimental studies performed in DMSO, which confirms this extended structure at the pendant (Figures 5b-5c).

Interestingly, in the VCD pattern of an extended structure for poly-(*S*)-Ala-(*R*)-MPA and poly-(*S*)-Ala-(*S*)-MPA is possible to observe the opposite orientation of the carbonyl band of the MPA (ca. 1670 cm^{-1}) due to their enantiomeric relationship (Figures 4b,c (DMSO) and Figure 5).

ECD studies were performed for these polymers in $CHCl_3$ and DMSO to determine how the conformational changes at the pendant affect to the helical sense excess of the polyene main chain. As expected, when the pendant group adopts an extended structure—poly-(*S*)-Ala-(*R*)-MPA and poly-(*S*)-Ala-(*S*)-MPA dissolved in DMSO—, the helical sense is induced by the chiral residue closest in sequence to the polyene backbone, in this case the alanine group (Figure 6a). As a result, an *M* helical sense is induced in poly-(*S*)-Ala-(*R*)-MPA and poly-(*S*)-Ala-(*S*)-MPA even though the absolute configuration of the second chiral residue, i.e., MPA, is different in both. On the contrary, when these studies are carried out in $CHCl_3$, a helical sense inversion happens when the absolute configuration of MPA changes (Figure 6b). This outcome confirms the activation of the chiral overpass effect in $CHCl_3$ due to the presence of a bent structure in the pendant. Similar effects were obtained for the enantiomeric series poly-(*R*)-Ala-(*R*)-MPA and poly-(*R*)-Ala-(*S*)-MPA, with opposite helicities induced in the PPAs due to the enantiomeric relationships (see S22 and S23).

Next, the total control of the chiral overpass effect was explored by playing with the conformational composition of the MPA moiety while the alanine fragment remains in a bent structure. To do that it is necessary to have two solvents that do not disrupt the intra-pendant hydrogen bond of alanine, but at the same time possess different polarities to play with the *antiperiplanar*/*synperiplanar* conformational equilibrium of the MPA moiety. Thus, while an *antiperiplanar* conformation is favoured in low-polar

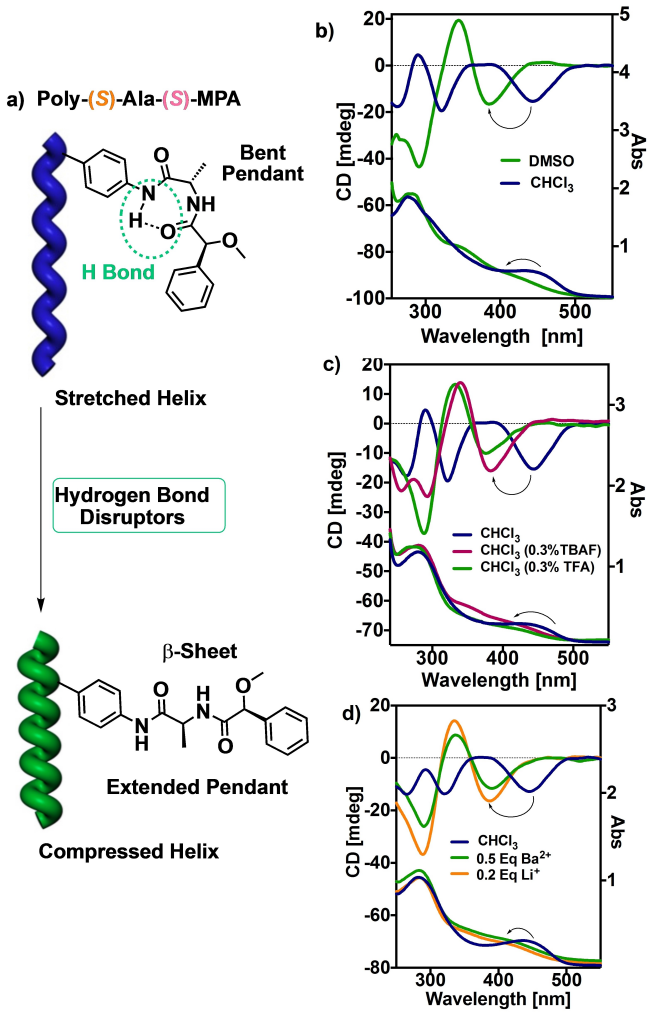

Figure 3. a) Conceptual representation of the conformational manipulation from bent to stretched pendant group of poly-(*S*)-Ala-(*S*)-MPA. ECD/UV/Vis and spectroscopy monitoring of the above process triggered by b) polar effects, c) hydrogen bond disruptors (TFA/TBAF) and d) metal coordination.

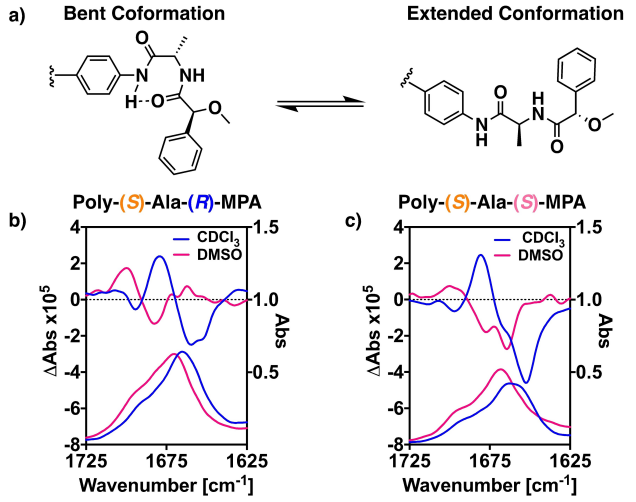

Figure 4. a) Conceptual representation of bent and extended conformations in the pendant groups. VCD/IR spectroscopy monitoring the dichroic inversion related to the conformational switch triggered by polar effects of b) poly-(*S*)-Ala-(*R*)-MPA and c) of poly-(*S*)-Ala-(*S*)-MPA.

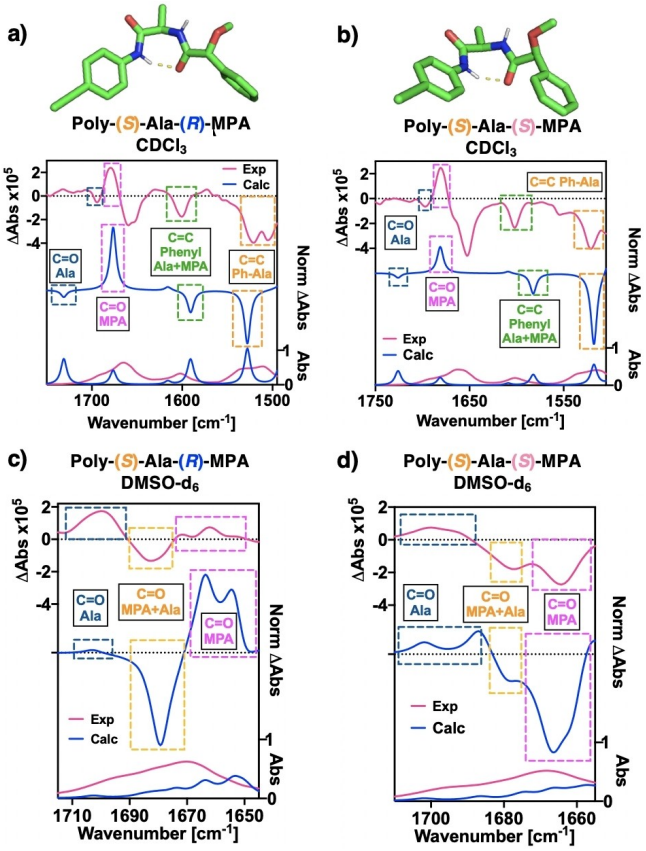

Figure 5. a) and b) Computed structures for bent conformations (γ-turn) of m-(*S*)-Ala-(*R*)-MPA and m-(*S*)-Ala-(*S*)-MPA and comparison of experimental vs calculated VCD/IR spectra with the corresponding polymers poly-(*S*)-Ala-(*R*)-MPA and poly-(*S*)-Ala-(*S*)-MPA in $CDCl_3$. c) and d) Computed vs experimental VCD/IR spectra of the extended conformation of poly-(*S*)-Ala-(*R*)-MPA and poly (*S*)-Ala-(*S*)-MPA in DMSO-d_6.

solvents, an increase in the solvent polarity favors the adoption of a *synperiplanar* conformation in this fragment. To achieve this goal, $CHCl_3$ was chosen as low-polar solvent while cyclohexanone and acetone were selected as polar solvents. ECD and UV/Vis studies of poly-(*S*)-Ala-(*R*)-MPA and poly-(*S*)-Ala-(*S*)-MPA in these solvents indicate the presence of a scaffold with similar elongation but opposite helical sense (Figure 7). Thus, a positive ECD band centered at 448 nm was obtained for poly-(*S*)-Ala-(*R*)-MPA in $CHCl_3$ indicating the adoption of a *P* helix by the polyene backbone, while a negative band is obtained for poly-(*S*)-Ala-(*R*)-MPA in acetone or cyclohexanone, indicative of an *M* helicity (Figure 7a).[26]

This helical inversion is a consequence of a conformational change in the MPA fragment, from *antiperiplanar* ($CHCl_3$) to *synperiplanar* (acetone or cyclohexanone), which places its aromatic ring in different orientations, producing the inversion. In the case of poly-(*S*)-Ala-(*S*)-MPA, the results were the opposite, showing a negative ECD band

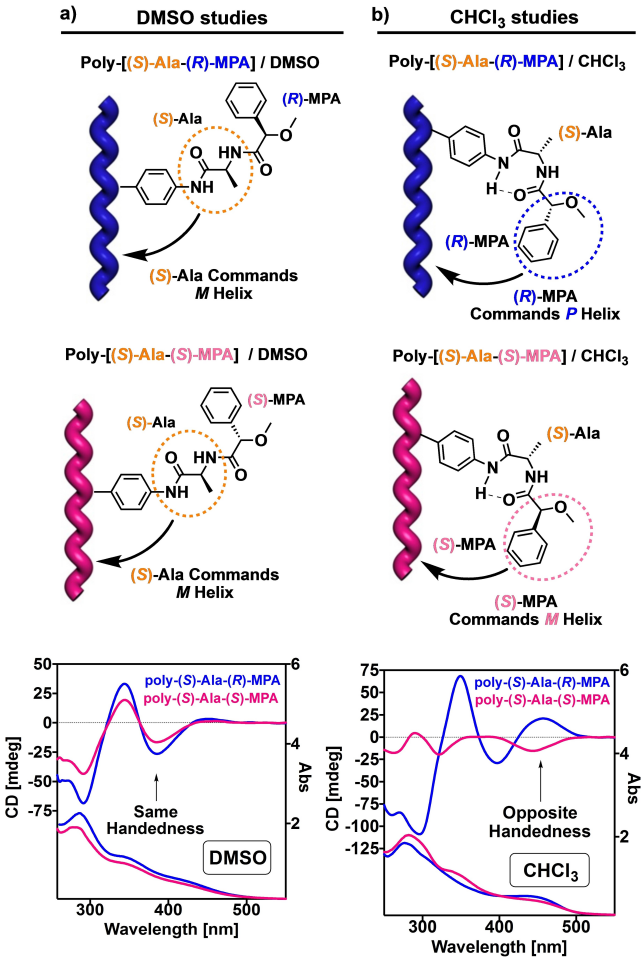

Figure 6. Conceptual representation and ECD spectra of the activation and deactivation of the chiral overpass effect by controlling the presence of a) an extended (DMSO) conformation or b) a bent conformation (γ-turn, $CHCl_3$) in the pendants of poly-(*S*)-Ala-(*R*)-MPA and poly-(*S*)-Ala-(*S*)-MPA.

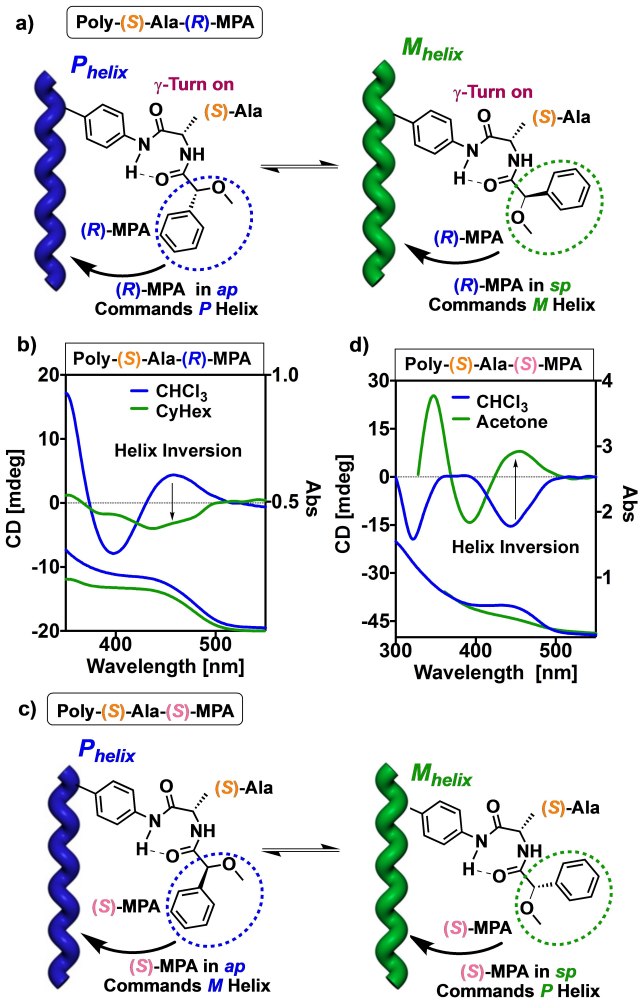

Figure 7. Conceptual representation of the chiral overpass induction by conformational modulation of the second chiral center monitored by ECD/UV/Vis spectra of a–b) poly-(*S*)-Ala-(*R*)-MPA and c–d) poly-(*S*)-Ala-(*S*)-MPA (CyHex and acetone, respectively).

centered at 448 nm when dissolved in $CHCl_3$ (*M* helix), while a positive band (*P* helix) is obtained when dissolved in acetone or cyclohexanone (Figure 7d). These studies were also carried out for the enantiomeric series—poly-(*R*)-Ala-(*R*)-MPA and poly-(*R*)-Ala-(*S*)-MPA (Figures S22 and S23)—obtaining, as expected, a total control of the helix, inducing *P* and *M* helices in the PPA by a total control of the chiral overpass effect. Moreover, it should be noted that poly-(*S*)-Ala-(*R*)-MPA and poly-(*R*)-Ala-(*R*)-MPA have identical behavior, inducing a *P* helix in $CHCl_3$ and a *M* helix in acetone. In turn, polymers poly-(*S*)-Ala-(*S*)-MPA and poly-(*R*)-Ala-(*S*)-MPA showed opposite helical sense inductions, *M* helix in $CHCl_3$ and *P* helix in acetone, due to the opposite configuration of the second chiral residue (MPA) (Figure 7).

Finally, we proceeded to do the structural elucidation of the polymers using atomic force macroscopy (AFM) and the information previously obtained from Raman, DSC, IR, ECD and VCD studies. AFM allowed us to directly visualize the macromolecular helical structures adopted by the polymers[27] following the protocol developed by the groups of Yashima[28] and Percec.[29] High-resolution AFM images were obtained from dilute solutions of poly-(*S*)-Ala-(*S*)-MPA (0.05 mg mL^{-1}, $CHCl_3$) and poly-(*S*)-Ala-(*S*)-MPA/Li^+ complex in 1/1 (mol/mol) ratio that were spin coated onto freshly cleaved highly oriented pyrolytic graphite (HOPG). These images showed, as expected, the presence of a compressed poly-(*S*)-Ala-(*S*)-MPA/Li^+ complex and a stretched helical scaffold for poly-(*S*)-Ala-(*S*)-MPA (Figures 8, S25 and S26). In both cases, *cis-transoidal* scaffolds were obtained with *P* orientation of the external helix and *M* orientation of the internal one. These helices showed different helical pitches and packing angles. Thus, values of 4.8 nm and 50° were obtained for poly-(*S*)-Ala-(*S*)-MPA/Li^+ complex (compressed helix), while 5.8 nm and 40° were obtained for poly-(*S*)-Ala-(*S*)-MPA (stretched helix).

Combining all the structural date allowed us to construct *cis-transoidal* helical structures with dihedral angles between conjugated double bonds of $\omega_1 = -160°$ and $\omega_1 = -170°$ for the compressed and stretched helices, and where the internal

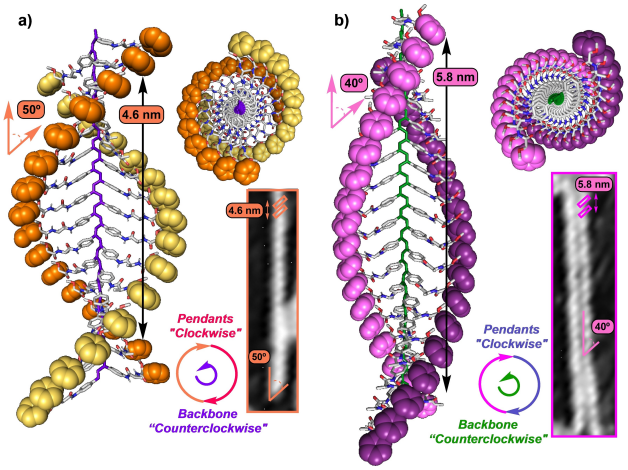

Figure 8. AFM Images and 3D-models of a) compressed and b) stretched *P* helices of poly-(*S*)-Ala-(*S*)-MPA obtained from $CHCl_3$ and $CHCl_3/Li^+$ solutions (HPOG as substrate).

and external helices rotate in opposite directions (P_{ext}/M_{int}).[27b]

Conclusion

In conclusion, this work demonstrates how the chiral overpass induction effect can be totally tamed, by introducing in the pendant groups of PPAs two chiral residues, which show independent and selective conformational control. As a result, it is possible to selectively induce an excess of *P* or *M* helical sense in the PPA main chain by varying the conformational composition at the second chiral residue through a chiral overpass effect. This polymer switch is achieved by a thorough design of the monomeric repeating unit. In our case, an alanine residue in either (*R*) or (*S*) configuration was introduced to link the pendant group to the PPA backbone through an anilide linkage and to play between an extended and a bent structure due to a conformational control in this group. Moreover, a second chiral residue consisting of (*R*)- or (*S*)-methoxyphenyl acetic acid was added to the pendant through the N-terminus of the alanine. This second chiral residue shows a conformational composition between two major conformers that places the bulkiest substituent, phenyl, in opposite directions and will allow the helical sense of the PPA to be controlled by means of a chiral overpass effect that occurs when alanine adopts a bent structure. As a result, when alanine adopts an extended structure, the second chiral residue is placed far from the polyene backbone. Thus, the helical sense adopted by the PPA is commanded by the chirality of the alanine, while changes in the absolute configuration of the second chiral center or conformational changes at this residue does not affect the helical sense of the PPA. In contrast, when alanine adopts a bent structure, both conformational changes and changes in the absolute configuration of the MPA moiety result in a helix inversion in the PPA. This fact indicates that a total control of chiral overpass effect is achieved.

To our knowledge, this is the first time that a chiral overpass effect has been tamed, making it possible to induce both helical senses in the PPA by changes in the conformational composition of the second chiral residue (MPA). As a remarkable result, three different helices are produced in the PPA by varying the conformational composition in the monomer repeating unit. This unique and novel helical sense control portrayed here opens promising prospects in advanced helical sense control of PPAs and can be applied to develop new multi-stimuli responsive chiral polymeric materials with enhanced applications as sensors, as chiroptical switches or in chiral recognition, among many others. Efforts in those directions are currently underway in our laboratory.

Acknowledgements

We thank financial support from AEI (PID2019-109733GB-I00), Ministerio de Ciencia e Innovación (PID2019-107307RB-100 and PID2020-117605GB-100). Xunta de Galicia (ED431 C 2018/30, ED431 C 2021/40, Centro Singular de Investigación de Galicia acreditación 2019–2022, ED431G 2019/03 and the European Regional Development Fund (ERDF), JSPS KAKENHI (Grant-in-Aid for Specially Promoted Research, No. 18H05209 (K.M.) and Grant-in-Aid for Scientific Research (A), No. 21H04691(K.M.) and the World Premier International Research Center Initiative (WPI), MEXT, Japan are gratefully acknowledged. We also thank Centro de Supercomputación de Galicia (CESGA) for computational resources. M. F.-M. thanks MICINN for a FPI contract (PID2019-109733GB-100).

Conflict of Interest

The authors declare no conflict of interest.

Data Availability Statement

The data that support the findings of this study are available in the supplementary material of this article.

Keywords: AFM · Chiral Overpass · Chirality · Chiroptical Switches · Helical Polymers

[1] a) V. Percec, Q. Xiao Bull, *Bull. Chem. Soc. Jpn.* **2021**, *94*, 900–928; b) V. Percec, Q. Xiao, *Isr. J. Chem.* **2021**, *61*, 530–556; c) V. Percec, *Isr. J. Chem.* **2020**, *60*, 48–66; d) E. Yashima, N. Ousaka, D. Taura, K. Shimomura, T. Ikai, K. Maeda, *Chem. Rev.* **2016**, *116*, 13752–13990; e) Z. Yu, S. Hecht, *Chem. Commun.* **2016**, *52*, 6639–6653; f) B. A. F. Le Bailly, J. Clayden, *Chem. Commun.* **2016**, *52*, 4852–4863; g) E. Schwartz, M. Koepf, H. J. Kitto, R. J. M. Nolte, A. E. Rowan, *Polym. Chem.* **2011**, *2*, 33–43; h) H. Iida, E. Yashima, *Synthesis and Application of Helical Polymers with Macromolecular Helicity Memo-*

ry, in Polymeric Chiral Catalyst Design and Chiral Polymer Synthesis (Ed.: S. Itsuno), Wiley, Hoboken, **2011**, ch. 7, p. 201; i) E. Yashima, K. Maeda, H. Iida, Y. Furusho, K. Nagai, *Chem. Rev.* **2009**, *109*, 6102–6211; j) E. Yashima, K. Maeda, Y. Furusho, *Acc. Chem. Res.* **2008**, *41*, 1166–1180; k) I. Huc, *Eur. J. Org. Chem.* **2004**, 17–29.

[2] a) T. Ikai, M. Ando, M. Ito, R. Ishidate, N. Suzuki, K. Maeda, E. Yashima, *J. Am. Chem. Soc.* **2021**, *143*, 12725–12735; b) M. Ando, R. Ishidate, T. Ikai, K. Maeda, E. Yashima, *J. Polym. Sci. Part A* **2019**, *57*, 2481–2490; c) D. Taura, S. Hioki, J. Tanabe, N. Ousaka, E. Yashima, *ACS Catal.* **2016**, *6*, 4685–4689; d) H. Iida, Z. Tang, E. Yashima, *J. Polym. Sci. Part A* **2013**, *51*, 2869–2879; e) Z. Tang, H. Iida, H.-Y. Hu, E. Yashima, *ACS Macro Lett.* **2012**, *1*, 261–265; f) R. P. Megens, G. Roelfes, *Chem. Eur. J.* **2011**, *17*, 8514–8523.

[3] a) S. Wang, S. Xie, H. Zeng, H. Du, J. Zhang, X. Wan, *Angew. Chem. Int. Ed.* **2022**, *61*, e202202268; *Angew. Chem.* **2022**, *134*, e202202268; b) K. Maeda, D. Hirose, M. Nozaki, Y. Shimizu, T. Mori, K. Yamanaka, K. Ogino, T. Nishimura, T. Taniguchi, M. Moro, E. Yashima, *Sci. Adv.* **2021**, *7*, abg5381; c) E. Anger, H. Iida, T. Yamaguchi, K. Hayashi, D. Kumano, J. Crassous, N. Vanthuyne, C. Roussel, E. Yashima, *Polym. Chem.* **2014**, *5*, 4909–4914; d) K. Maeda, D. Hirose, N. Okoshi, K. Shimomura, Y. Wada, T. Ikai, S. Kanoh, E. Yashima, *J. Am. Chem. Soc.* **2018**, *140*, 3270–3276; e) K. Maeda, E. Yashima, *Top. Curr. Chem.* **2017**, *375*, 72; f) A. C. Pauly, P. Theato, *Macromol. Rapid Commun.* **2013**, *34*, 516–521; g) E. Yashima, K. Maeda, *Macromolecules* **2008**, *41*, 3–12; h) K. Maeda, E. Yashima, *Top. Curr. Chem.* **2006**, *265*, 47.

[4] a) L. Zhang, H.-X. Wang, S. Li, M. Liu, *Chem. Soc. Rev.* **2020**, *49*, 9095–9120; b) R. Rodríguez, E. Quiñoá, R. Riguera, F. Freire, *Chem. Mater.* **2018**, *30*, 2493–2497.

[5] a) T. Ikai, T. Kurake, S. Okuda, K. Maeda, E. Yashima, *Angew. Chem. Int. Ed.* **2021**, *60*, 4625–4632; *Angew. Chem.* **2021**, *133*, 4675–4682; b) R. Ishidate, T. Sato, T. Ikai, S. Kanoh, E. Yashima, K. Maeda, *Polym. Chem.* **2019**, *10*, 6260–6268; c) D. Hirose, A. Isobe, E. Quiñoá, F. Freire, K. Maeda, *J. Am. Chem. Soc.* **2019**, *141*, 8592–8598; d) K. Shimomura, T. Ikai, S. Kanoh, E. Yashima, K. Maeda, *Nat. Chem.* **2014**, *6*, 429–434.

[6] a) B. Nieto-Ortega, R. Rodríguez, S. Medina, E. Quiñoá, R. Riguera, J. Casado, F. Freire, J. Ramírez, *J. Phys. Chem. Lett.* **2018**, *9*, 2266–2270; b) S. Hecht, *Mater Today* **2005**, *8*, 48–55.

[7] S. Mishra, A. Kumar, E. Z. B. Smolinsky, R. Naaman, K. Maeda, T. Nishimura, T. Taniguchi, T. Yoshida, K. Takayama, E. Yashima, *Angew. Chem. Int. Ed.* **2020**, *59*, 14671–14676; *Angew. Chem.* **2020**, *132*, 14779–14784.

[8] a) J. J. Tarrío, R. Rodríguez, B. Fernández, E. Quiñoá, F. Freire, *Angew. Chem. Int. Ed.* **2022**, *61*, e202115070; *Angew. Chem.* **2022**, *134*, e202115070; b) W. Zheng, T. Ikai, E. Yashima, *Angew. Chem. Int. Ed.* **2021**, *60*, 11294–11299; *Angew. Chem.* **2021**, *133*, 11394–11399; c) S. Wang, D. Hu, X. Guan, S. Cai, G. Shi, Z. Shuai, J. Zhang, Q. Peng, X. Wan, *Angew. Chem. Int. Ed.* **2021**, *60*, 21918–21926; *Angew. Chem.* **2021**, *133*, 22089–22097; d) L. Xu, C. Wang, Y. X. Li, X. H. Xu, L. Zhou, N. Liu, Z. Q. Wu, *Angew. Chem. Int. Ed.* **2020**, *59*, 16675–16682; *Angew. Chem.* **2020**, *132*, 16818–16825; e) K. Maeda, M. Nozaki, K. Hashimoto, K. Shimomura, D. Hirose, T. Nishimura, G. Watanabe, E. Yashima, *J. Am. Chem. Soc.* **2020**, *142*, 7668–7682; f) K. Dhbaibi, C. Shen, M. Jean, N. Vanthuyne, T. Roisnel, M. Górecki, B. Jamoussi, L. Favereau, J. Crassous, *Front. Chem.* **2020**, *8*, 2–9.

[9] a) T. Leigh, P. Fernandez-Trillo, *Nat. Chem. Rev.* **2020**, *4*, 291–310; b) M. S. Kaucher, M. Petarca, A. E. Dulcey, A. J. Kim, S. A. Vinogradov, D. A. Hammer, P. A. Heiney, V. Percec, *J. Am. Chem. Soc.* **2007**, *129*, 11698–11699; c) V. Percec, A. E. Dulcey, V. S. K. Balagurusamy, Y. Miura, J. Smidrkal, M. Peterca, S. Nummelin, U. Edlund, S. D. Hudson, P. A. Heiney, H. Duan, S. N. Magonov, S. A. Vinogradov, *Nature* **2004**, *430*, 764–768.

[10] J. W. Y. Lam, B. Z. Tang, *Acc. Chem. Res.* **2005**, *38*, 745–754.

[11] a) S. Leiras, E. Suárez-Picado, E. Quiñoá, R. Riguera, F. Freire, *Giant* **2021**, *7*, 100068; b) Y. Song, S. Kang, S. Kang, Y. Lee, *Angew. Chem. Int. Ed.* **2020**, *59*, 22968–22972; *Angew. Chem.* **2020**, *132*, 23168–23172; c) V. Percec, J. G. Ruick, M. Peterca, P. A. Heiney, *J. Am. Chem. Soc.* **2008**, *130*, 7503–7508; d) S. Leiras, F. Freire, J. M. Seco, E. Quiñoá, R. Riguera, *Chem. Sci.* **2013**, *4*, 2735–2743; e) K. Maeda, H. Mochizuki, M. Watanabe, E. Yashima, *J. Am. Chem. Soc.* **2006**, *128*, 7639–7650; f) K. Maeda, N. Kamiya, E. Yashima, *Chem. Eur. J.* **2004**, *10*, 4000–4010.

[12] a) K. Cobos, R. Rodríguez, O. Domarco, B. Fernández, E. Quiñoá, R. Riguera, F. Freire, *Macromolecules* **2020**, *53*, 3182–3193; b) R. Rodríguez, E. Quiñoá, R. Riguera, F. Freire, *J. Am. Chem. Soc.* **2016**, *138*, 9620–9628.

[13] a) F. Freire, J. M. Seco, E. Quiñoá, R. Riguera, *Angew. Chem. Int. Ed.* **2011**, *50*, 11692–11696; *Angew. Chem.* **2011**, *123*, 11896–11900; b) V. Percec, E. Aqad, M. Peterca, J. G. Rudick, L. Lemon, J. C. Ronda, B. B. De, P. A. Heiney, E. W. Meijer, *J. Am. Chem. Soc.* **2006**, *128*, 16365–16732.

[14] a) X. Guan, S. Wang, G. Shi, J. Zhang, X. Wan, *Macromolecules* **2021**, *54*, 4592–4600; b) T. Van Leeuwen, G. H. Heideman, D. Zhao, S. J. Wezenberg, B. L. Feringa, *Chem. Commun.* **2017**, *53*, 6393–6396; c) M. Alzubi, S. Arias, I. Louzao, E. Quiñoá, R. Riguera, F. Freire, *Chem. Commun.* **2017**, *53*, 8573–8576; d) I. Louzao, J. M. Seco, E. Quiñoá, R. Riguera, *Angew. Chem. Int. Ed.* **2010**, *49*, 1430–1433; *Angew. Chem.* **2010**, *122*, 1472–1475.

[15] a) Z. Fernández, B. Fernández, E. Quiñoá, F. Freire, *J. Am. Chem. Soc.* **2021**, *143*, 20962–20969; b) R. Rodríguez, E. Suárez-Picado, E. Quiñoá, R. Riguera, F. Freire, *Angew. Chem. Int. Ed.* **2020**, *59*, 8616–8622; *Angew. Chem.* **2020**, *132*, 8694–8700; c) N. Zhu, K. Nakazono, T. Takata, *Chem. Commun.* **2016**, *52*, 3647–3649; d) V. Percec, J. G. Rudick, M. Petarca, M. Wagner, M. Obata, C. M. Mitchell, W.-D. Cho, V. S. K. Balagurusamy, P. A. Heiney, *J. Am. Chem. Soc.* **2005**, *127*, 15257–15264.

[16] a) G. Shi, Y. Li, X. Dai, J. Shen, X. Wan, *Chirality* **2022**, *34*, 574–586; b) Y. Kamikawa, T. Kato, H. Onouchi, D. Kashiwagi, K. Maeda, E. Yashima, *J. Polym. Sci. Part A* **2004**, *42*, 4580–4586; c) J. J. L. M. Cornelissen, J. J. J. M. Donners, R. De Gelder, W. S. Graswinckel, G. A. Metselaar, A. E. Rowan, N. A. J. M. Sommerdijk, R. J. M. Nolte, *Science* **2001**, *293*, 676–680; d) J. J. L. M. Cornelissen, A. E. Rowan, R. J. M. Nolte, N. A. J. M. Sommerdijk, *Chem. Rev.* **2001**, *101*, 4039–4070.

[17] E. Suárez-Picado, E. Quiñoá, R. Riguera, F. Freire, *Angew. Chem. Int. Ed.* **2020**, *59*, 4537–4543; *Angew. Chem.* **2020**, *132*, 4567–4573.

[18] R. Rodríguez, E. Quiñoá, R. Riguera, F. Freire, *Small* **2019**, *15*, 1805413.

[19] a) Z. Fernández, B. Fernández, E. Quiñoá, R. Riguera, F. Freire, *Chem. Sci.* **2020**, *11*, 7182–7187; b) M. Fukuda, R. Rodríguez, Z. Fernández, T. Nishimura, D. Hirose, G. Watanabe, E. Quiñoá, F. Freire, K. Maeda, *Chem. Commun.* **2019**, *55*, 7906–7909.

[20] Deposition numbers 2180644 and 2180647 contain the supplementary crystallographic data for this paper. These data are provided free of charge by the joint Cambridge Crystallographic Data Centre and Fachinformationszentrum Karlsruhe Access Structures service.

[21] a) N. S. L. Tan, A. B. Lowe, *Angew. Chem. Int. Ed.* **2020**, *59*, 5008–5021; *Angew. Chem.* **2020**, *132*, 5040–5053; b) Z. Ke, S. Abe, T. Ueno, K. Morokuma, *J. Am. Chem. Soc.* **2011**, *133*, 7926–7941.

[22] C. I. Simionescu, V. Percec, S. Dumitrescu, *J. Polym. Sci. Polym. Chem. Ed.* **1977**, *15*, 2497–2509.
[23] a) C. I. Simionescu, V. Percec, *Prog. Polym. Sci.* **1892**, *8*, 133–214; b) H. Shirakawa, T. Ito, S. Ikeda, *Polym. J.* **1973**, *4*, 460–462.
[24] L. Liu, T. Namikoshi, Y. Zang, T. Aoki, S. Hadano, Y. Abe, I. Wasuzu, T. Tsutsuba, M. Teraguchi, T. Kaneko, *J. Am. Chem. Soc.* **2013**, *135*, 602–605.
[25] a) M. A. Martínez, A. Doncel-Giménez, J. Cerdá, J. Calbo, R. Rodríguez, J. Aragó, J. Crassous, E. Ortí, L. Sánchez, *J. Am. Chem. Soc.* **2021**, *143*, 13281–13291; b) E. E. Greciano, R. Rodríguez, K. Maeda, L. Sánchez, *Chem. Commun.* **2020**, *56*, 2244–2247; c) K. Maeda, T. Miyagawa, A. Furuko, H. Onouchi, E. Yashima, *Macromolecules* **2015**, *48*, 4281–4293; d) Y. Hase, K. Nagai, K. Maeda, N. Ochi, K. Sawaba, K. Sakajiri, K. Okoshi, E. Yashima, *J. Am. Chem. Soc.* **2009**, *131*, 10719–10732.
[26] a) B. Fernández, R. Rodríguez, E. Quiñoá, R. Riguera, F. Freire, *ACS Omega* **2019**, *4*, 5233–5240; b) B. Fernández, R. Rodríguez, A. Rizzo, E. Quiñoá, R. Riguera, F. Freire, *Angew. Chem. Int. Ed.* **2018**, *57*, 3666–3670; *Angew. Chem.* **2018**, *130*, 3728–3732.
[27] a) A. Yurtsever, S. Das, T. Nishimura, R. Rodríguez, D. Hirose, K. Miyata, A. Sumino, T. Fukuma, K. Maeda, *Chem. Commun.* **2021**, *57*, 12266–12269; b) F. Freire, E. Quiñoá, R. Riguera, *Chem. Commun.* **2017**, *53*, 481–492; c) R. Rodríguez, J. Ignés-Mullol, F. Sagués, E. Quiñoá, R. Riguera, F. Freire, *Nanoscale* **2016**, *8*, 3362–3367.
[28] a) J. Kumaki, *Polym. J.* **2016**, *48*, 3–14; b) E. Yashima, *Polym. J.* **2010**, *42*, 3–16; c) J. Kumaki, S.-I. Sakurai, E. Yashima, *Chem. Soc. Rev.* **2009**, *38*, 737–746; d) S. Sakurai, K. Okoshi, J. Kumaki, E. Yashima, *J. Am. Chem. Soc.* **2006**, *128*, 5650–5651; e) S.-I. Sakurai, K. Okoshi, J. Kumaki, E. Yashima, *Angew. Chem. Int. Ed.* **2006**, *45*, 1245–1248; *Angew. Chem.* **2006**, *118*, 1267–1270.
[29] a) V. Percec, J. G. Rudick, M. Peterca, S. R. Staley, M. Wagner, M. Obata, C. M. Mitchell, W.-D. Cho, V. S. K. Balagurusamy, J. N. Lowe, M. Glodde, O. Weichold, K. J. Chung, N. Ghionni, S. N. Magonov, P. A. Heiney, *Chem. Eur. J.* **2006**, *12*, 5731–5746; b) V. Percec, J. G. Rudick, M. Wagner, M. Obata, C. M. Mitchell, W.-D. Cho, S. N. Magonov, *Macromolecules* **2006**, *39*, 7342–7351.

Manuscript received: July 7, 2022
Accepted manuscript online: September 19, 2022
Version of record online: October 13, 2022